

Label-Free Quantitative Proteome Analysis of Skeletal Tissues Under Mechanical Load

Wei-Bing Zhang and Lin Wang*

Department of Cellular and Developmental Biology, Institute of Stomatology, Nanjing Medical University, Nanjing, China

ABSTRACT

Skeletal tissue has the capability to adapt its mass and structure in response to mechanical stress. However, the molecular mechanism of bone and cartilage to respond to mechanical stress are not fully understood. A label-free quantitative proteome approach was used for the first time to obtain a global perspective of the response of skeletal tissue to mechanical stress. Label-free quantitative analysis of 1D-PAGE-LC/MS/MS based proteomics was applied to identify differentially expressed proteins. Differential expression analysis in the experimental groups and control group showed significant changes for 248 proteins including proteins related to proliferation, differentiation, regulation of signal transduction and energy metabolic pathways. Fluorescence labeling by incorporation of alizarin/calcein in newly formed bone minerals qualitatively demonstrated new bone formation. Skeletal tissues under mechanical load evoked marked new bone formation in comparison with the control group. Bone material apposition was evident. Our data suggest that 39 proteins were assigned a role in anabolic process. Comparisons of anabolic versus catabolic features of the proteomes show that 42 proteins were related to catabolic. In addition, some proteins were related to regulation of signal transduction and energy pathways, such as tropomyosin 4, fibronectin 1, and laminin, might be new molecular targets that are responsive to mechanical force. Differentially expressed proteins identified in this model may offer a useful starting point for elucidating novel aspects of the effects of mechanical force on skeletal tissue. *J. Cell. Biochem.* 108: 600–611, 2009. © 2009 Wiley-Liss, Inc.

KEY WORDS: LABEL-FREE QUANTITATIVE PROTEOMICS; MASS SPECTROMETRY; BONE; CARTILAGE; MECHANICAL LOADING

Steoarthritis and osteoporosis are very common degenerative diseases. Although major progress has been made in the field of these diseases in recent years, there is still no cure for most severe skeletal diseases and adequate treatment is not readily available because of the lack of thorough understanding of their pathogenesis. Mechanical stress is an important epigenetic factor for the regulation of remodeling of skeletal tissues including bone and cartilage. Mechanically induced cellular alterations are major contributors to pathological conditions [Raisz, 1999]. Osteopenia or osteoporosis is caused by lack of physiological mechanical loading, and moderate physical exercise is critical for maintaining bone integrity and architecture [Faibis et al., 2006]. Skeletal diseases can be defined by a failure of the body's adaptive response that maintains tissue structure needed to withstand daily loading. Understanding the molecular basis skeletal tissue response to

mechanical stimuli should help identify new approaches for the treatment of musculoskeletal diseases and injuries.

Proteins present in bone and cartilage tissue are essential for all life processes and are critical final products of the information pathways. Profiling these proteins is vital for a thorough understanding of mechanobiology. Proteome analysis offers great opportunities because of its ability to focus on simultaneous changes in a large number of proteins, which may help reveal the interplay of different events at a given time. However, proteome research on bone has mainly focused on *in vitro* systems using osteoblasts [Wang et al., 2004], osteoclasts [Czupalla et al., 2006], or chondrocytes [Piltti et al., 2008] to identify proteins that are expressed by a cell type under given experimental conditions. However, using these systems, the actual protein profile of bone cannot be established. Chondrocytes, osteoblasts, and osteoclasts all

All authors have no conflicts of interest.

Additional Supporting Information may be found in the online version of this article.

Grant sponsor: National Natural Science Foundation of China; Grant number: 30572068; Grant sponsor: Nanjing Medical University; Grant number: NY0527.

*Correspondence to: Prof. Lin Wang, Department of Cellular and Developmental Biology, Institute of Stomatology, Nanjing Medical University, Nanjing, China. E-mail: zhangweibing@vip.sina.com

Received 13 May 2009; Accepted 29 June 2009 • DOI 10.1002/jcb.22291 • © 2009 Wiley-Liss, Inc.

Published online 10 August 2009 in Wiley InterScience (www.interscience.wiley.com).

participate and interact with each other in regulating skeletal remodeling processes in response to mechanical stimuli. In fact, a tight network exists among the different cell types in bone including cells in bone marrow. Thus *in vivo* stimuli may likely cause simultaneous, interplaying responses in the various cell types rather than an isolated response in a specific cell type. Therefore, comprehensive information and knowledge of the proteome of bone and cartilage response to mechanical stress *in vivo* is essential for understanding the role of mechanical stimuli in regulating skeletal remodeling processes.

To obtain better insights into proteome analysis of bone and cartilage response to mechanical stress *in vivo*, we have conducted studies of midpalatal suture expansion [Ma et al., 2008]. The midpalatal suture, located between the maxillary bones in the palate, contains secondary cartilage that is highly responsive to various mechanical forces [Hou et al., 2007]. The mid-palatal suture is a unique model for investigating the mechanical modulation of both bone and cartilage remodeling. We separated extracted proteins by 2D gel electrophoresis (2DE), and proteins within the gels were identified by mass spectrometer (MS). Comparative proteomic analysis showed increases in 22 protein spots that were present in the midpalatal suture expansion group [Ma et al., 2008]. However, the analysis of extreme proteins (extremely basic or acidic, extremely small or big, extremely hydrophobic) presented a substantial challenge for 2DE. Shotgun proteomics, which is a high-throughput proteome analysis approach, could avoid the intrinsic limitations of 2DE [Xie et al., 2006]. Until now, large-scale comprehensive identification of proteins has not been attempted in any studies on the response of bone and cartilage to mechanical stress.

The objective of this study was to use a midpalatal suture expansion model, one-dimensional polyacrylamide gel electrophoresis (1D-PAGE) sample fractionation with liquid chromatography-tandem mass spectrometry (LC/MS/MS)-based protein identification and label-free quantitation to identify profile proteins in intact skeletal tissues that are regulated by mechanical force. The overall effect of mechanical force on intact skeletal tissues was observed *in vivo* to gain an initial insight into the most relevant effects of mechanical force at the protein level. Our experimental procedure successfully identified 248 differentially expressed proteins that are regulated by mechanical force in skeletal tissues.

MATERIALS AND METHODS

ANIMALS AND TREATMENT

Six-week-old male C57BL/6 mice were randomly divided into an experimental group and a control group. For histological analysis, 24 mice were allocated to four experimental groups that were treated with an applied expansion force for different time periods: 1, 3, 7, or 14 days with 6 mice for each time point, including 3 with midpalatal suture expansion and 3 serving as controls (non-operated). Expansive wires with opening loops were applied to the experimental animals under pentobarbital anesthesia. The expansive force applied to the mid-palatal suture was mediated by the bilateral molars with the use of 0.014-in. stainless steel orthodontic wire

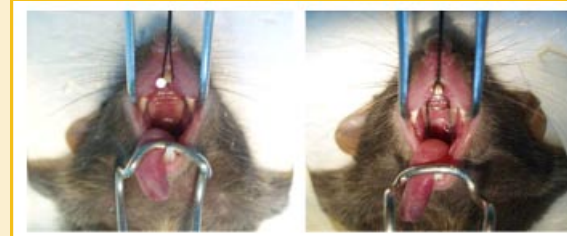


Fig. 1. Mid-palatal suture expansion in mice. Experimental/expansion maxilla with the opening loop bonded to the first and second molars (right) and non-operated control (left). [Color figure can be viewed in the online issue, which is available at www.interscience.wiley.com.]

(GAC International, Inc.). The appliances were bonded to first and second maxillary molars on both sides by a light cured adhesive (3M Unitek) using a method reported in previous studies [Hou et al., 2007]. Control mice underwent anesthesia without wire application (Fig. 1). In addition, at day 3, 12 mice from each group were used for one-dimensional polyacrylamide gel electrophoresis (1-DE). For micro-CT analysis, six mice were studied at day 14, including three with mid-palatal suture expansion and three serving as controls. Six mice were used for fluorescence bone labeling studies with three for control and three for expansion at day 14. Animals had access to food pellets and fresh water *ad libitum*. All procedures were approved by the Ethics Committee at Nanjing Medical University, China.

HISTOLOGY

A half of specimens were selected at days 1, 3, 7, and 14 and fixed overnight with fixative with 4% (w/v) paraformaldehyde in 0.1 M phosphate-buffered saline solution. The fixed specimens were demineralized in 0.5 M ethylenediaminetetra-acetic acid (EDTA) for 14 days at 4°C and then embedded in paraffin, sectioned at 7 μ m intervals, and stained with hematoxylin and eosin, and then microphotographs were taken.

MICRO-CT

Micro-CT (GE Healthcare, Canada) was used for scanning as well as for morphometric analysis. The intact maxillae were placed in a holder and scanned with the palate perpendicular to the image plane producing a 3D stack of images or volume. The scanned volume had a voxel resolution of 8 μ m. 3D morphometric analysis was performed by selecting the palatal bone regions to obtain the bone volume fraction mineralized bone was separated from bone marrow with a marching cube 3D segmentation algorithm in which the grayscale images were segmented using a 3D Gaussian filter (with mean = 0.8 and filter support = 1) to remove noise, and threshold analysis were calculated with Microview (GE Healthcare). We used the auto-threshold method because it segregates mineralized tissue based on the distribution for a given specimen of background and mineralized voxels and helps to reduce experimental error associated with temporal effects.

FLUORESCENCE LABELING AND SAMPLE PROCESSING

Mice were given an intraperitoneal injection of calcein (Sigma) at 6 mg/kg body weight on day 1 the opening loops were applied and alizarin complexone (Sigma) at 60 mg/kg body weight on day 14. Control mice were given the fluorochrome dyes at the same time. Mice were sacrificed 2 days after the second dye injection, and the maxillae were harvested for analysis. The specimens were fixed with 4% (w/v) paraformaldehyde and dehydrated in a series of graded alcohols before embedded in Osteo-Bed resin (Polysciences, Inc., Warrington, PA) following manufacturer's instruction. Frontal sections of 140 μ m were cut with a low speed saw (Buehler, Lake Bluff, IL) and mounted on slides using mounting medium (Electron Microscopy Sciences, Hatfield, PA). The sections were viewed in a Confocal microscopy (An Olympus Fluoview 500 confocal scanning unit, Japan).

TISSUE EXTRACTION

Based on a previous report [Hou et al., 2007; Ma et al., 2008], the health status of the mice in the midpalatal suture expansion group was evaluated by monitoring daily body weights for 3 days. We chose to perform the proteomic analysis of the midpalatal sutures 3 days after the operation to identify proteins that might be responsible for the observed structural changes. The mice were euthanized as described above, and the midpalatal suture tissues were dissected and stored on ice. The fresh tissue specimens were trimmed free of soft tissue and washed with ice-cold 0.01 M PBS buffer solution to remove contaminants, and then ground into powder in liquid nitrogen. The tissue powder was ground in a lysis buffer [NaCl: 0.439 g; NP-40: 500 μ l; sodium deoxycholate: 0.5 g; 10% SDS: 500 μ l; Na₃PO₄: 0.19 g; EDTA: 0.029 g; NaF: 0.105 g; H₂O: 50 ml and a Complete Protease Inhibitor Cocktail Tablet (Roche); pH 7.2]. Subsequently, the powder was incubated for 12 h at 4°C. The supernatant was collected after centrifugation. Protein concentrations were determined using Bradford protein assays (Bio-Rad).

IDENTIFICATION OF PROTEIN BY LC-MS/MS

Proteins (200 μ g) were separated by 10% SDS-PAGE (Fig. 2). The bands containing proteins were cut into 10 slices. Each slice was digested with trypsin and analyzed by LC-MS/MS. The LC-MS/MS

system consisted of a quaternary pump, an autosampler, and a Finnigan LTQ-ORBITRAP mass spectrometer (Thermo Electron, San Jose, CA) equipped with a nanospray source. Each digest was analyzed three times by LC-MS/MS, and data analysis was based on the cumulative total proteins identified in three replicate analyses. Assignment of MS/MS data was performed using SEQUEST (Bioworks 3.2, Thermo Electron) and X! Tandem searches against the International Protein Index (IPI) database (mouse, 2008 December version) from the European Bioinformatics Institute (EBI) and against a randomized version of the IPI database for calculation of false-positive rates (FPR). Reversed sequences were appended to the database for the evaluation of FPR. Cysteine residues were searched as static modifications of 57.0215 Da, and methionine residues were searched as variable modifications of +15.9949 Da. Peptides were searched using fully tryptic cleavage constraints, and up to two missing cleavage sites were allowed for tryptic digestion. The mass tolerances were 2 Da for parent masses and 1 Da for fragment masses, respectively. The peptides were considered as positive identification if their Xcorr was higher than 1.9 for singly charged peptides, 2.2 for doubly charged peptides, and 3.75 for triply charged peptides, respectively, and if Δ Cn cutoff values were \geq 0.22. FPR were calculated by using the following equation, $FPR = 2^*n(\text{rev})/(n(\text{rev}) + n(\text{forw}))$, where n(forw) and n(rev) were the number of peptides identified in proteins with forward (normal) and reversed sequence, respectively. A FPR less than 5% was obtained for the peptide identifications by using above parameters. We accepted the returned protein identifications when Mascot scores were above the statistically significant threshold ($P < 0.05$) and if at least two peptides matched the identified protein.

RELATIVE PROTEIN QUANTITATION

A label-free proteome quantitation method was used as described previously [Gao et al., 2008]. Three measurements (spectral counting, ion intensity, and peak area) were used for protein quantitation. Spectral counting for each protein was calculated using MS Result Manager based on SEQUEST and X! Tandem search results. Quantitation by ion intensity and peak area were performed on the peptide sequences filtered by MS Result Manager and extracted from MS data.

WESTERN BLOT ANALYSIS

Extracted proteins were separated by SDS-PAGE and immunoblotted using primary antibodies against fibronectin 1, tropomyosin 4 (Abcam, US), osteoglycin, and annexin A4 (Santa Cruz, CA). β -actin was used as a loading control. The separated proteins were incubated overnight with primary antibodies. The blots were then incubated with peroxidase-conjugated secondary antibody (1:2,000). Protein bands were visualized using an enhanced chemiluminescence system (Supersignal West Pico Trial Kit, Pierce, Rockford), and the density of each band was quantified with a Fluor-S MultiImager (Bio-Rad). The experiment was performed with samples from six mice in each group, and the mean expression level for each protein was calculated accordingly.

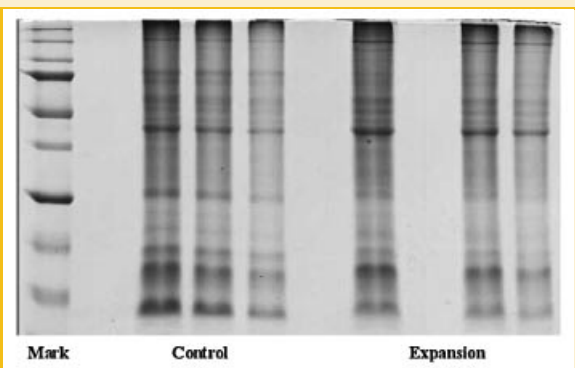


Fig. 2. Electrophoretic profiles of skeletal tissues proteomes on 1D gels.

GO MINER ANALYSIS

The Go Miner program was used to classify the identified proteins, which provided a general view of protein location and function [Zeeberg et al., 2003].

PATHWAY ANALYSIS BY PATHWAYSTUDIO™

An analysis of cellular processes influenced by up/down-regulated proteins in force-treated skeletal tissue was performed using PathwayStudio software (v4.00, Ariadne Genomics, Rockville, MA) [Nikitin et al., 2003]. This text-mining software uses a database of molecular networks that are assembled from scientific abstracts and a manually created dictionary of synonyms to recognize biological terms [Nikitin et al., 2003]. The cellular processes influenced by various treatments were determined by searching the database for imported genes/proteins and for cellular processes in which the imported genes/proteins are involved. In our analysis, each identified cellular process was confirmed manually using the relevant Pub Med/Medline hyperlinked abstracts.

STATISTICS

All experiments were repeated at least three times. Differences between treatment and control groups were analyzed using Student's *t*-tests. Values of $P < 0.05$ were considered statistically significant. Results were expressed as fold change (mean \pm SEM) compared to values for the control group.

RESULTS

GENERAL OBSERVATIONS

The animals tolerated the expansion without complications. The mice with activated opening loops (expansion) had a modest weight loss on days 1 and 3, but regained weight such that there were no differences in weights at later time points between expansion and control animals.

PALATAL SUTURE MORPHOLOGY ANALYSIS

Results from micro-CT analysis at day 14 showed that the midpalatal suture was expanded following application of an activated opening loop (Fig. 3). Three-dimensional micro-CT reconstruction of expansion maxillae exhibited a high degree of sutural separation evoked by expansive force. A trapezoidal-shaped opening of the midpalatal suture more widen at the oral than at the nasal side of the suture.

Histologically, the midpalatal suture of non-expansion groups consisted mainly of cartilage, that is, two masses of chondrocytes covering the edges of palatal bones, separated from each other by a thin layer of fibrous tissue (Fig. 4A). During the experimental period, the suture in expansion groups underwent minor changes related to normal growth with a decrease in the number of chondrocytes and an increase in the amount of fibrous tissue (Fig. 4F,G). In the experimental groups with activated loops, the midpalatal suture was expanded and the collagen fibers were reoriented across the suture (compare Fig. 4A–C with Fig. 4E–G). At the same time, periosteal cells started to migrate into the suture. The chondrocytes decreased

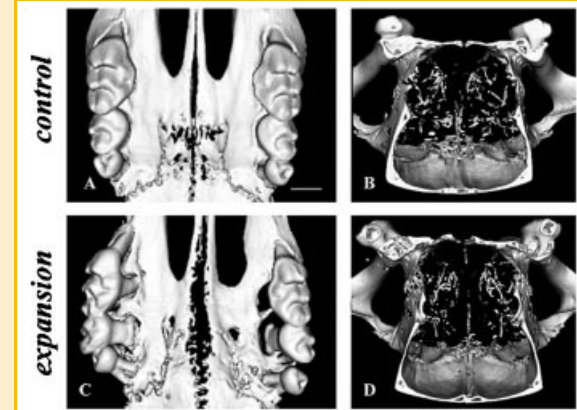


Fig. 3. Three-dimensional micro-CT reconstruction of control and expansion maxillae. Occlusal view of reconstructed maxillae of control (A) and expansion (C). Coronal plane view in the first molars of reconstructed maxillae of control (B) and expansion (D). Scale bar (A): 1.0 mm. The midpalatal suture width of expansion specimens increased significantly.

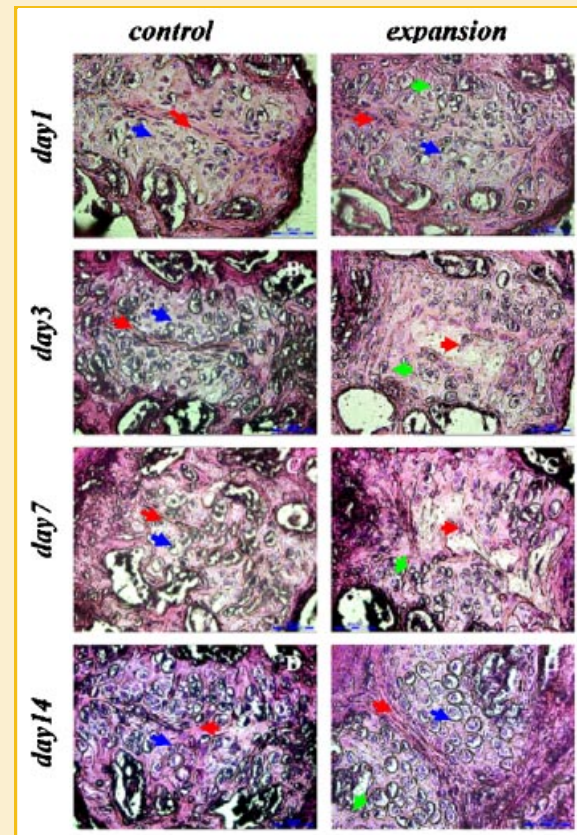


Fig. 4. Hematoxylin and eosin staining of frontal sections of midpalatal sutures of control (A–D) and expansion animals (E–H) at days 1, 3, 7, and 14. In the experimental groups with activated loops, the midpalatal suture was expanded and the collagen fibers were reoriented across the suture (compare Fig. 4A–C with Fig. 4E–G). No inflammatory cells were observed within the suture of the experimental groups. Scale bar (A–H): 50 μ m. Red arrow—fibers, blue arrow—chondrocyte, green arrow—periosteal cells. [Color figure can be viewed in the online issue, which is available at www.interscience.wiley.com.]

in numbers and formed only 1–2 layers at this stage (Fig. 4F). Bone formation was initially observed at the edges of the palatal bones at day 7 (Fig. 4G). At day 14, a cellular fibrous tissue filled the suture, and regeneration of the original layered structure (Fig. 4H). During the experimental period, no inflammatory cells were observed in the suture area.

FLUORESCENCE LABELING OF NEWLY MINERALIZED BONE

Fluorescence labeling by incorporation of alizarin/calcein in newly formed bone minerals qualitatively demonstrated new bone formation. We labeled bone surfaces by injecting mice with calcein and alizarin complexone at the beginning and end of a 14-day expansion period. The mid-palatal suture edge area of animals treated for 14 days with the opening loop was filled with alizarin-positive material, separating the calcein-labeled original edges of the palatal bones. Tensile force loading of the mid-palatal suture evoked marked new bone formation in comparison with the control group (Fig. 5).

1-DE-LC/MS/MS AND PROTEIN IDENTIFICATION

To identify mechanical force-regulated proteins in skeletal tissues, we compared the global protein expression pattern of the treatment group with that of the control group. To increase the confidence level of protein identification, a minimum of two peptides for the identification of each protein was used as filtering criterion. The false-positive rate at the protein level decreased to 0.48%. After applying this stringent criterion, 835 unique proteins expressed in both the treatment group and the control group were identified (see Supplemental Material). Combining values of $P < 0.05$ and fold changes ≥ 2 or ≤ 0.5 for the filtering criterion, 248 differentially expressed proteins were identified with high confidence.

To gain a better understanding of the differentially expressed proteins identified in skeletal tissues, the Go Miner program was used to classify these proteins.

SUBCELLULAR LOCATION

In total, 211 differentially expressed proteins were annotated in subcellular locations (Fig. 6A). The intracellular locations of the identified proteins are shown in Figure 6B. As illustrated, the majority of the identified proteins (46.2%) originated from the cytoplasm. The next two significant locations were the mitochondrion (17.5%) and the cytoskeleton (12.4%) (Fig. 6A). In addition, 26 membrane proteins were also identified (Table I).

PROTEIN ROLE ASSIGNMENT

Two hundred thirteen differentially expressed proteins were described by protein function. A graphical representation of identified proteins based on their known physiological functions is presented in Figure 6C. The largest subgroup of proteins was assigned to binding function. One hundred thirty-nine of the identified proteins were engaged in catalytic activity, and another

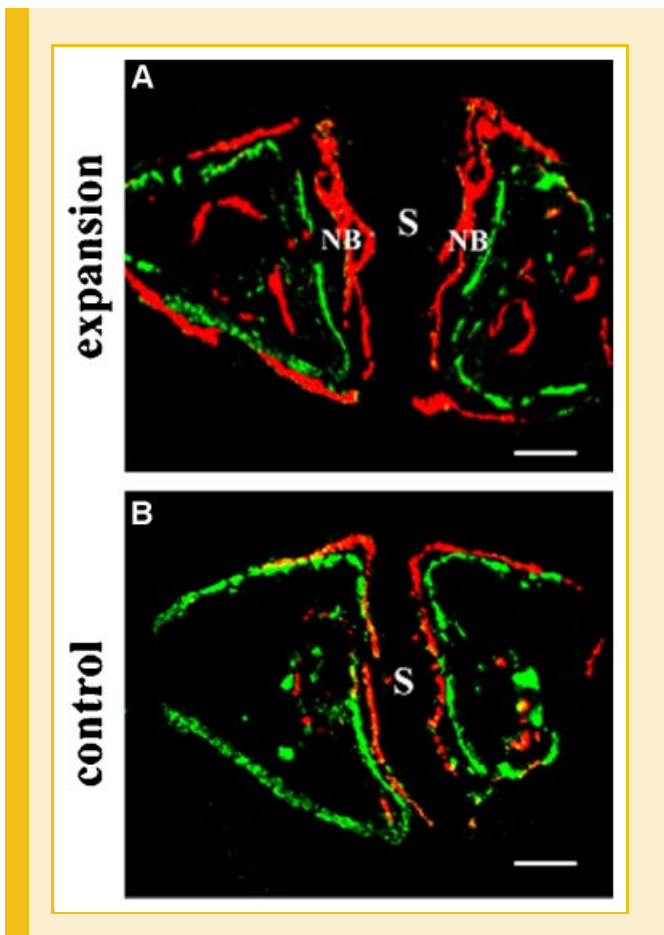


Fig. 5. Representative photomicrographs of newly formed sutural bone double-labeled in the mid-palatal suture of the control and expansion at day 14. Calcein-labeled bone surfaces are in green and alizarin complexone-labeled surfaces are red. A: Expansion of the mid-palatal suture. B: Control of the mid-palatal suture under normal growth. S, suture; NB, new bone. Areas of newly mineralized bone are indicated by red fluorescence. The specimens treated with expansive force demonstrated greater amount of alizarin complexone uptake and therefore a great amount of bone apposition in expansion group comparison with control group. Scale bar (A and B): 50 μ m, respectively. [Color figure can be viewed in the online issue, which is available at www.interscience.wiley.com.]

25 proteins were classified as their regulators. This result indicates that 164 unique proteins identified from the bone proteome related to enzymatic activity. These digestive enzymes had to be strongly regulated to prevent unwanted proteolysis. Indeed, the 13 protease inhibitors that were identified were endopeptidase inhibitors (Table I). In addition, one kinase inhibitor (tyrosine 3-monooxygenase), one phospholipase inhibitor (annexin A4), and one protein kinase regulator (protein kinase, camp-dependent regulatory, type I, alpha) were identified. Finally, 13 signal transduction proteins were identified (Table I).

In total, 18 structural proteins were identified that contained 5 structural constituents of the cytoskeleton, 3 ECM structural constituents, and 2 structural constituents of bone. Moreover, some low-abundance proteins associated with important functions such as protein biosynthesis were identified in the proteome analysis of mouse bone, which included eight transcription regulator proteins

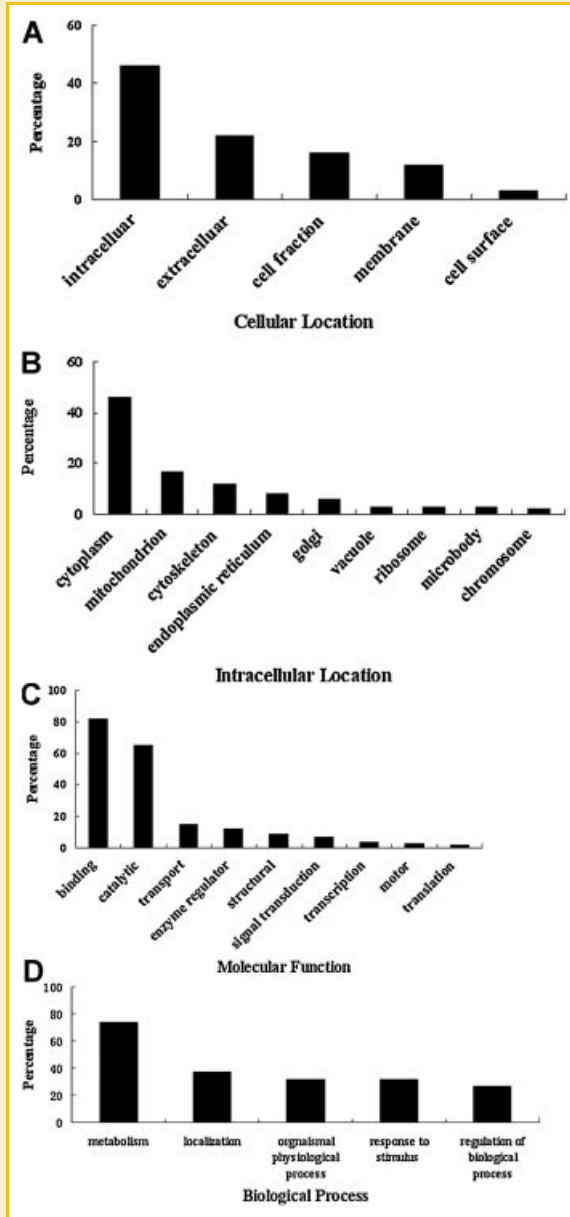


Fig. 6. Cellular distribution of differentially expressed proteins that are regulated by mechanical force in skeletal tissues. **A:** The cellular compartment distribution. **B:** The intracellular component distribution. **C:** Functional distribution of differentially expressed proteins that are regulated by mechanical force in skeletal tissues. **D:** Biological process distribution of differentially expressed proteins that are regulated by mechanical force in skeletal tissues.

the identified proteins involved in different biological process categories is shown in Figure 6D. The largest number of proteins belonged to the category describing metabolism and was composed of 149 proteins. This broad category contained many of the above-mentioned enzymes, notably proteases, as well as enzymes involved in basic cellular processes such as protein catabolism. Among these proteins, 39 proteins were assigned a role in anabolic process. Comparisons of anabolic versus catabolic features of the proteomes show that 42 proteins were related to catabolic (Table I). A large group of 65 proteins was assigned a role in organismal physiological processes. Among these proteins, seven bone remodeling proteins (fibronectin 1, osteoglycin, apolipoprotein A-I, laminin beta 2, xanthine dehydrogenase, apolipoprotein A-I binding protein, fibrinogen gamma polypeptide) were identified. In the third largest group, 65 proteins associated with responses to stimulus activity were observed. This group was categorized into four types: response to biotic stimulus (14 proteins), response to endogenous stimulus (9 proteins), response to external stimulus (31 proteins), and response to stress (42 proteins). Besides proteins involved in the above-mentioned biological processes, there were 75 and 55 proteins involved in the biological processes of localization and regulation, respectively.

WESTERN BLOTTING ANALYSIS TO VERIFY PROTEIN LEVEL CHANGES

Western blot analysis was performed to validate the label-free quantitative proteome analysis results. Based on the availability of antibodies, we selected and analyzed four proteins (tropomyosin 4, fibronectin 1, osteoglycin, annexin A4) that were high-expressed in force-treated skeletal tissue. β -actin was used as an internal control. The results confirmed the differential protein expression observed by 1-DE-LC/MS/MS (Fig. 7).

FUNCTIONAL ANNOTATION OF PROTEINS DIFFERENTIALLY EXPRESSED PROTEINS IN FORCE-TREATED SKELETAL TISSUE

More detailed analysis of cellular processes influenced by these 248 proteins was performed using Pathway Studio software, an automated text-mining tool that generates pathways from entries in the PubMed database as well as in other public sources. We determined that 32 proteins have been well-documented in osteoblasts; 185 proteins may be involved in many key processes related to differentiation and proliferation events according to their well-documented functions in chondrocytes, osteoblasts, and osteoclasts. The results are expressed graphically in Figure 8: for example, within the events of mechanical force-induced skeletal remodeling process, proteins involved in processes such as cell survival, apoptosis, and regulation of signal transduction, locomotion, differentiation, and proliferation were indicated. Forty-seven proteins primarily functions in many key changes were related to the regulation of signal transduction events. Eighty-nine proteins were related to proliferation and 96 proteins to differentiation, respectively. Eighty-six proteins were related to apoptosis and 69 proteins to cell survival, respectively. Nine proteins were related to locomotion events (Fig. 8).

(CAP—adenylate cyclase-associated protein 1, sepiapterin reductase, histidine-rich glycoprotein, prohibitin, adenylosuccinate synthetase, prolactin-induced protein, Ras suppressor protein 1, UDP-glucose pyrophosphorylase 2) and two translational regulator molecules (eukaryotic translation initiation factor 6, poly(rC) binding protein 1).

BIOLOGICAL PROCESS

In total, 202 identified proteins were described by the biological process in which they were involved. The classification of

TABLE I. Functional Classification of Proteins Identified by MS

Abbreviation	NCBI GI	Full name of closed identified protein	P-value	Fold change
Membrane				
Cox4i1	6753498	Cytochrome c oxidase subunit iv isoform 1	0.001	0.265
Spnb-2	117938332	Spectrin beta 2 isoform 1	8.07E-05	0.368
Orm1	6679182	Orosomucoid 1	0.00015	2.002
Vdac1	6755963	Voltage-dependent anion channel 1	0.0013	2.005
2310001A20Rik	21313668	Riken cdna 2310001a20	0.0075	2.007
Oat	8393866	Ornithine aminotransferase	0.0024	2.042
Nid2	84370361	Nidogen 2	0.004	2.059
Clic1	15617203	Chloride intracellular channel 1	0.0012	2.068
Mpz	162139829	Myelin protein zero	5.84E-05	2.079
Gc	51172612	Group specific component	0.003	2.127
Ehbpb1	154240710	eh domain binding protein 1	0.0008	2.244
Atp1a1	21450277	na+/k+-atpase alpha 1 subunit	0.0024	2.251
Dock1	88853584	Dicator of cytokinesis 1	0.0022	2.284
Anpep	6678664	Alanyl (membrane) aminopeptidase	0.0027	2.376
Tor1aip1	21450141	Torsin a interacting protein 1	0.0045	2.447
Erlin2	23956396	er lipid raft associated 2	0.0013	2.666
uqcrfs1	13385168	Ubiquinol-cytochrome c reductase, rieske iron-sulfur polypeptide 1	0.0017	2.688
Dsg3	110625833	Desmoglein 3	0.0014	2.882
Eno2	7305027	Enolase 2, gamma neuronal	0.00062	2.943
Heph	110815853	Ceruloplasmin isoform a	0.0087	2.982
Palm2	27777697	Paralemmin 2	0.00082	3.272
Lrg1	16418335	Leucine-rich alpha-2-glycoprotein	3.57E-05	4.633
Vdac2	6755965	Voltage-dependent anion channel 2	5.29E-07	7.877
Ugt1a10	145864477	udp glycosyltransferase 1 family, polypeptide a10	0.003	7.927
Sec14l3	71480138	sec14-like 3	3.15E-05	8.837
VMtx2	31543274	Metaxin 2	2.58E-05	20.169
Protease inhibitor				
Mup5	113930708	Major urinary protein 5	3.80E-05	0.222
Pebp1	84794552	Phosphatidylethanolamine binding protein 1	0.00018	0.319
Clic1	15617203	Chloride intracellular channel 1	0.0012	2.069
Serpina3a	51092274	Serine (or cysteine) proteinase inhibitor, clade b (ovalbumin), member 3a	0.0032	2.077
Thbs1	47059073	Thrombospondin 1	0.0041	2.091
Psma5	7106387	Proteasome (prosome, macropain) subunit, alpha type 5	2.64E-05	2.198
Ngp	164519050	Neutrophilic granule protein	0.00087	2.415
BC048546	75677551	cdna sequence bc048546	0.00056	2.585
Hrg	16716461	Histidine-rich glycoprotein	0.0048	3.142
Itih3	159110717	Inter-alpha trypsin inhibitor, heavy chain 3	0.0032	3.316
Serpina3c	160333613	Serine (or cysteine) proteinase inhibitor, clade b, member 3c	0.00028	3.321
Cfb	6996919	Complement factor b	0.00036	4.142
Serpina1a	130503301	Serine (or cysteine) proteinase inhibitor, clade a, member 3n	2.96E-05	4.234
Signal transduction				
Traf1	13385998	tnf receptor-associated protein 1	0.0337	0.464
S100a9	6677837	s100 calcium binding protein a9	0.0055	2.049
Anxa9	145864497	Annexin a9	0.0075	2.066
Clic1	15617203	Chloride intracellular channel 1	0.00117	2.069
Thbs1	47059073	thrombospondin 1	0.0041	2.091
Car3	31982861	Carbonic anhydrase 3	0.0095	2.233
Anpep	6678664	Alanyl (membrane) aminopeptidase	0.0028	2.376
Mapk14	10092590	Mitogen-activated protein kinase 14	0.0011	3.152
Gnao1	164607137	Guanine nucleotide binding protein, alpha o isoform b	0.0006	3.258
Car2	157951596	Carbonic anhydrase 2	0.00199	3.784
Hp	8850219	Haptoglobin	0.00142	3.868
Cfb	6996919	Complement factor b	0.00036	4.142
Plcd1	97790167	Phospholipase c, delta 1	0.0297	8.956
Biosynthetic				
Asns	33469123	Asparagine synthetase	0.0413	0.369
Got2	6754036	Glutamate oxaloacetate transaminase 2, mitochondrial	1.74E-06	0.476
2310001A20Rik	21313668	Riken cdna 2310001a20	0.0075	2.007
Ccbl1	31982063	Cysteine conjugate-beta lyase 1	0.0051	2.019
S100a9	6677837	s100 calcium binding protein a9	0.0055	2.049
Fdps	19882207	Farnesyl diphosphate synthetase	0.0047	2.083
Ugdh	6678499	udp-glucose dehydrogenase	0.01458	2.095
ATP5C1	163838648	atp synthase, h+ transporting, mitochondrial f1 complex, gamma subunit isoform b	0.004	2.099
Napr1	31982089	Nicotinate phosphoribosyltransferase domain containing 1	0.0042	2.119
Gc	51172612	Group specific component	0.003	2.127
Apoa1	160333304	Apolipoprotein a-i	0.007	2.139
Cmpk1	165377065	Ump-cmp kinase	0.0017	2.194
Atp5f1	20070412	atp synthase, h+ transporting, mitochondrial f1 complex, o subunit	0.0021	2.210
Pdixk	26006861	Pyridoxal (pyridoxine, vitamin b6) kinase	0.00098	2.219
Ckmt1	6753428	Creatine kinase, mitochondrial 1, ubiquitous	0.003	2.225
Adss	31560737	Adenylosuccinate synthetase, non-muscle	0.0019	2.235
Pccb	13385310	propionyl coenzyme a carboxylase, beta polypeptide	0.005	2.237
Atp1a1	21450277	na+/k+-atpase alpha 1 subunit	0.0024	2.252
Atp6v1f	21314824	Atpase, h+ transporting, lysosomal v1 subunit f	0.0225	2.284
Spr	160333789	Sepiapterin reductase	0.0004	2.289
Ndufa10	13195624	Nadh dehydrogenase (ubiquinone) alpha subcomplex 10	7.71E-05	2.296

(Continued)

TABLE I. (Continued)

Abbreviation	NCBI GI	Full name of closed identified protein	P-value	Fold change
Hmgcl	6680233	3-hydroxy-3-methylglutaryl-coenzyme a lyase	0.0019	2.303
Vars	34328204	Valyl-tRNA synthetase	0.0137	2.325
Adsl	29788764	adenylosuccinate lyase	0.002	2.387
Ndubf10	58037109	nadh dehydrogenase (ubiquinone) beta subcomplex, 100.00122.395		
Hprt1	96975138	Hypoxanthine guanine phosphoribosyl transferase 1	0.0006	2.399
Dia1	19745150	Diaphorase 1	0.013	2.530
Ak3	23956104	Adenylate kinase 3	0.0009	2.671
Adk	19527306	Adenosine kinase	0.0007	2.781
Gpd1	6753966	Glycerol-3-phosphate dehydrogenase 1 (soluble)	8.07E-05	2.930
Eno2	7305027	Enolase 2, gamma neuronal	0.0006	2.943
Ak1	10946936	Adenylate kinase 1	0.0009	2.9459
Psp	6679509	Parotid secretory protein	3.40E-06	3.249
Ugcgl1	45387933	udp-glucose ceramide glucosyltransferase-like 1	0.0033	3.281
Adh1	6724311	Alcohol dehydrogenase 1 (class i)	0.0003	3.340
Atp5o	78214312	atp synthase, h ⁺ transporting, mitochondrial f0 complex, subunit b, isoform 1	4.12E-05	3.397
Car2	157951596	Carbonic anhydrase 2	0.002	3.784
Eif6	27501448	Eukaryotic translation initiation factor 6	0.0001	5.123
Got1	160298209	Glutamate oxaloacetate transaminase 1, soluble	7.38E-05	5.192
Catabolic				
G6pd2	13937389	Glucose-6-phosphate dehydrogenase 2	2.32E-05	0.311
Myh6	6754774	Myosin, heavy polypeptide 6, cardiac muscle, alpha	0.004	0.469
Got2	6754036	Glutamate oxaloacetate transaminase 2, mitochondrial	1.74E-06	0.477
Hibadh	21704140	3-Hydroxyisobutyrate dehydrogenase precursor	0.0204	2.038
Oat	8393866	Ornithine aminotransferase	0.002	2.043
GalK	93102413	Galactokinase 1	0.014	2.053
Gale	30409988	Galactose-4-epimerase, udp	8.20E-05	2.131
Pnp	7305395	Purine-nucleoside phosphorylase	0.0016	2.133
Psma5	7106387	proteasome (prosome, macropain) subunit, alpha type 5	2.64E-05	2.198
Pdxk	26006861	Pyridoxal (pyridoxine, vitamin b6) kinase	0.00098	2.219
Pccb	13385310	Propionyl coenzyme a carboxylase, beta polypeptide	0.005	2.237
Atp1a1	21450277	na ⁺ /k ⁺ -atpase alpha 1 subunit	0.0024	2.252
Psmb4	45592932	Proteasome beta 4 subunit	0.0032	2.265
Rnh1	31981748	Ribonuclease/angiogenin inhibitor 1	0.0002	2.451
Dci	31981810	Dodecenoyl-coenzyme a delta isomerase (3,2 trans-enoyl-coenzyme a isomerase)	0.0022	2.462
Pgls	13384778	6-Phosphogluconolactonase	0.006	2.465
tal1	33859640	Transaldolase 1	0.0017	2.534
Psmb2	31981327	Proteasome (prosome, macropain) subunit, beta type 2	0.0016	2.643
Guad	6753960	Guanine deaminase	0.0013	2.650
Adh7	31560625	Alcohol dehydrogenase 7 (class iv), mu or sigma polypeptide	0.0003	2.657
Ldhb	6678674	Lactate dehydrogenase b	0.0001	2.699
Acadm	6680618	Acyl-coenzyme a dehydrogenase, medium chain	0.0004	2.735
Ech1	7949037	Enoyl coenzyme a hydratase 1, peroxisomal	0.0005	2.759
Gpd1	6753966	Glycerol-3-phosphate dehydrogenase 1	8.07E-05	2.930
Eno2	7305027	Enolase 2, gamma neuronal	0.0006	2.943
Psmb3	6755202	Proteasome beta 3 subunit	0.0009	2.994
Nt5c	7657031	5',3'-Nucleotidase, cytosolic	0.0097	3.086
Pgam1	114326546	Phosphoglycerate mutase 1	0.0008	3.134
Echs1	29789289	Enoyl coenzyme a hydratase, short chain, 1, mitochondrial	0.00075	3.251
Sae1	9790247	Sumo1 activating enzyme subunit 1	0.0029	3.317
Adh1	6724311	Alcohol dehydrogenase 1 (class i)	0.0003	3.340
Psm14	145966883	Proteasome (prosome, macropain) 26s subunit, non-atpase, 14	0.048	3.404
Psmd4	124248577	Proteasome 26s atpase subunit 4	0.0013	3.561
Txnr1	13569841	Thioredoxin reductase 1 isoform 2	0.0004	3.619
Car2	157951596	Carbonic anhydrase 2	0.002	3.784
Psma7	7106389	Proteasome (prosome, macropain) subunit, alpha type 7	0.0019	4.000
Psmb1	7242197	Proteasome (prosome, macropain) subunit, beta type 1	0.00014	4.156
Mpst	65301475	3-Mercaptopyruvate sulfurtransferase	0.0009	4.228
Got1	160298209	glutamate oxaloacetate transaminase 1, soluble	7.38E-05	5.192
CS	13385942	Citrate synthase	5.76E-06	5.624
Plcd1	9790167	Phospholipase c, delta 1	0.0297	8.956
Pgam2	9256624	Phosphoglycerate mutase 2	0.0001	10.54
Regulation of signal transduction				
Gstp2	32401425	Glutathione S-transferase, pi 2	0.00024	2.008
Fn1	46849812	Fibronectin 1	0.004	2.025
Lamb2	31982223	Laminin, beta 2	0.0042	2.176
Cdc10	8173550	Cell division cycle 10 homolog	0.00055	2.183
Cdc42	6753364	Cell division cycle 42	0.0002	2.688
TR	13569841	Thioredoxin reductase 1 isoform 2	0.0004	3.619
Cell motility				
Tpm4	47894398	Tropomyosin 4	0.0057	4.508
Bone remodeling				
Ogn	6679166	Osteoglycin	0.0015	2.177
Phospholipase inhibitor				
Anxa4	161016799	Annexin A4	3.95E-05	2.084

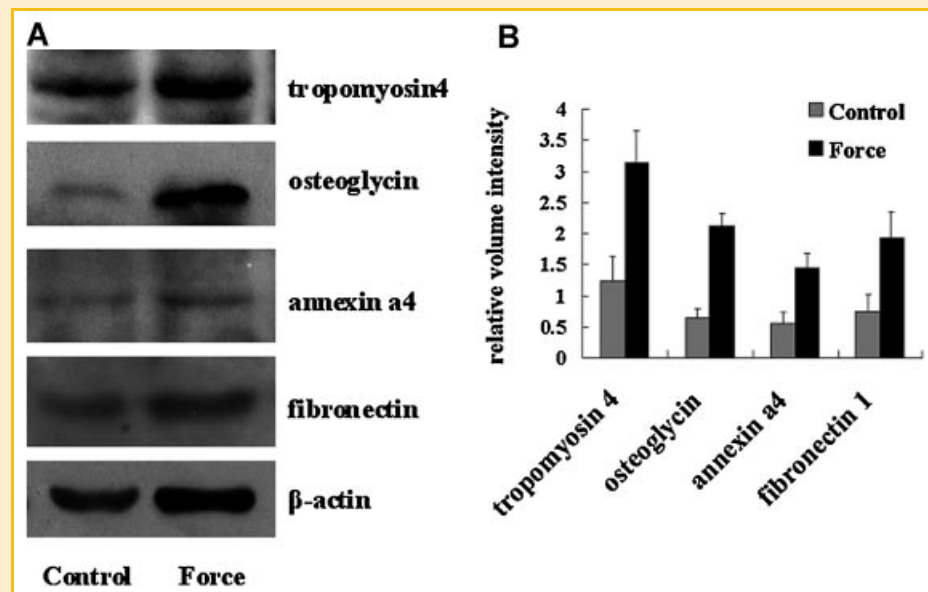


Fig. 7. Validation of the label-free quantitative proteomics results by Western blot. A: Western blot analyses with anti-tropomyosin 4, anti-fibronectin 1, anti-osteoglycin, anti-annexin A4, and anti- β -actin polyclonal antibodies were performed on 50–100 mg of total protein extracts prepared from force treatment group from control group. B: The bars represent the density of gel bands determined from two samples. The results are consistent with those results of the label-free quantitative proteomics.

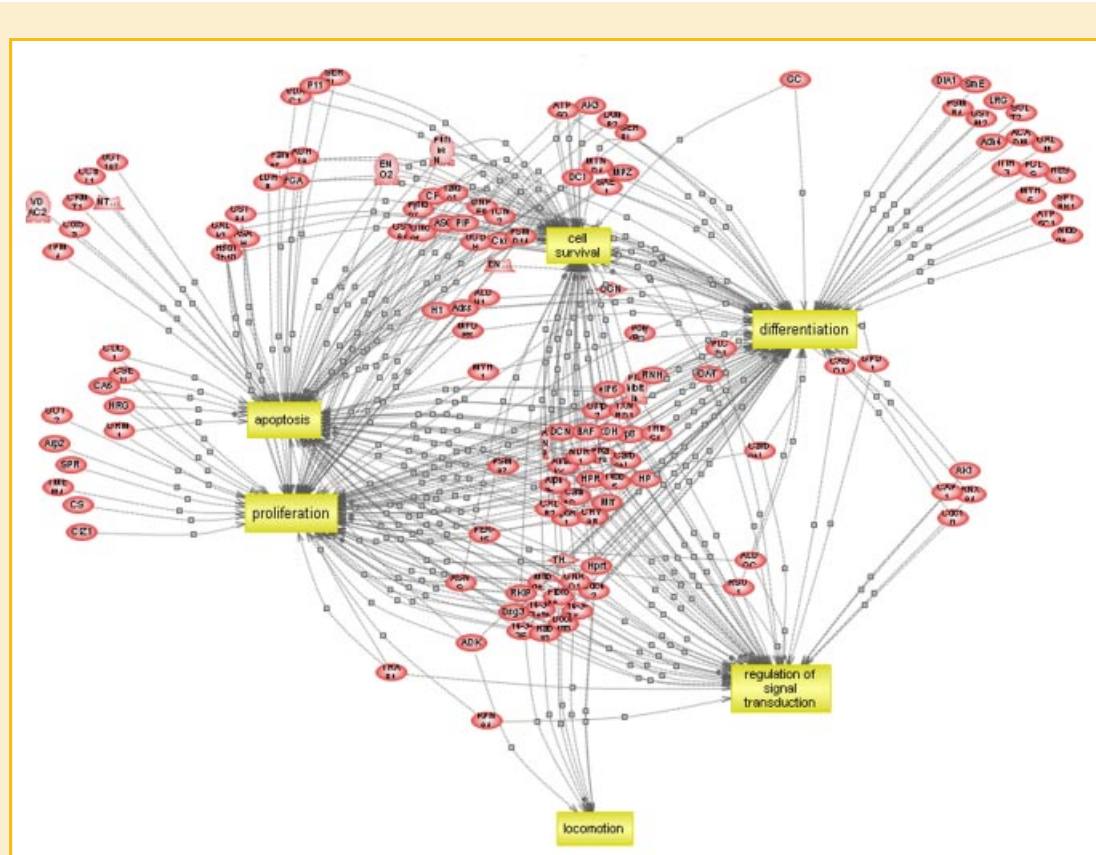


Fig. 8. Regulated pathways involving differentially expressed proteins in force-treated skeletal tissue as predicted by PathwayStudio software. One hundred forty-seven proteins are shown as ovals, and the regulated processes are represented by squares. Regulation events are displayed using arrows and documented by literature citations. A large number of identified proteins participate in regulating the skeletal remodeling process pathway. The references linked to each protein mined by this software are listed in Table S2 of Supporting Information. [Color figure can be viewed in the online issue, which is available at www.interscience.wiley.com.]

DISCUSSION

Bone models its mass and structure in response to mechanical strain [Huiskes et al., 2000]. Bone metabolism is a continuous, dynamic remodeling process that is normally maintained by a tightly coupled balance between osteoclast-mediated bone resorption and osteoblast-mediated bone formation. Mechanical stimuli play an important role in regulating bone growth, and tensional stress promotes bone formation. Moderate physical exercise is essential for maintaining bone integrity and prevents bone loss. However, the exact mechanism underlying the effects of exercise on skeletal tissues is not fully understood. When skeletal tissue is loaded, the mechanical force is transformed into a biological signal that triggers a series of biological events, such as chondrocyte hypertrophy, angiogenesis, cartilage and other tissue resorption, skeletal matrix formation, and matrix calcification. Finally, mechano-transduced osteogenesis occurs and new bone forms. Numerous proteins are involved in these processes, and there is an urgent need to identify and characterize these critical proteins. We have, for the first time, employed proteome analysis *in vivo* to search for novel pathways involved in the bone-sparing effect of mechanical force and found several novel stress-regulated proteins in intact skeletal tissue.

Mouse midpalatal suture expansion was used to study the ability of skeletal tissues to respond to mechanical stimulation. Expansion forces across the midpalatal suture promote bone resorption through activation of osteoclasts and bone and cartilage formation via increased proliferation and differentiation of periosteal cells. Our data indicate it is capable of expanding the suture of young mice by a significantly increased suture width. Results from micro-CT analysis at day 14 showed that the mid-palatal suture was expanded following application of an activated opening loop. We also found that expansive force across the mid-palatal suture promoted bone formation. Fluorescence labeling at day 14 showed that a large mass of new bone was formed within the suture area. Histological evaluation of several mid-palatal suture specimens showed that no inflammatory cells within the suture of the experimental animals. Our results suggest that the biological responses following mid-palatal suture expansion are likely induced by mechano-sensitive mechanisms rather than by wound healing processes. These original data demonstrated that mid-palatal suture expansion in mice we conducted is a successful model for the study of responses of bone and cartilage to mechanical force. In the present study, the mouse model was chosen also because, contrary to the paucity of proteomic databases applicable to some other animals such as dogs and cats, the availability of the mouse proteomic database allowed us to identify interesting proteins based on the MS results.

The goal of this study was to elucidate the changes in the proteome between non-stressed suture tissues and suture tissues subjected to mechanical stresses. The results of our quantitative analyses showed that the expression patterns of 248 proteins were significantly different between the force treatment group and the control group. Many bone-specific proteins were identified. For example, up-regulated creatine kinase was involved in bone growth and differentiation. Interestingly, the majority of identified

regulated proteins have not been previously associated with effects of mechanical stimuli on bone. Non-collagenous proteins made up only 10% of total bone protein content. Thus a majority of these biologically important proteins were relatively low natural abundance proteins. These identified proteins were differentially expressed and exhibited a broad spectrum of functions including the control of cell proliferation, cell-matrix interactions, and mediation of hydroxyapatite deposition.

Presumably, mechanical signal transduction is critical for normal physiological processes in bone cells including development, differentiation, and adaptation [Rubin et al., 2006]. Mechano-transduction refers to coupled mechanical and physicochemical events at the cell surface that convert mechanical stimuli into chemical stimuli. In our study, one kinase inhibitor (tyrosine 3-monooxygenase), one phospholipase inhibitor (annexin A4) and one protein kinase regulator (protein kinase, camp-dependent regulatory, type I, alpha) were identified, which were key elements of most signal transduction pathways that regulate cell physiology and pathology [Cravatt, 2005]. In addition, 14 signal transduction proteins were identified in our study. These proteins are likely involved in various processes of tissue remodeling within the mechanically expanded mid-palatal suture, although the underlying mechanism is still unclear. The membrane structure creates a complex association between the inner and outer leaflets, and transmembrane proteins are involved in stabilizing the coupling between resorption and formation. The organized membrane may have greater significance for mechanical response than for passing signals originating from liganded receptors. Furthermore, 26 membrane proteins were identified. Membrane proteins mediate many vital cellular processes and transfer metabolites and transmitted signals between cells and their environment, between organelles within the cell, and between organ systems.

These results suggest that a global approach of shotgun proteome analysis might be useful for identifying novel force-regulated pathways in bone. However, the proteomic strategy used in this study has some limitations. Despite their importance to cell function and the fact that roughly 20–30% of all open reading frames were predicted to encode membrane proteins, this class of proteins still presents a challenge for proteome analyses because of the difficulties in extraction, solubilization, and separation [Wu and Yates, 2003].

PathwayStudio software was used in this study, which includes an automated text-mining tool that can generate pathways for well-documented proteins from the entire PubMed database and from other public sources [Nikitin et al., 2003; Pollard et al., 2006]. This analysis has provided many insights into the function of differentially expressed proteins during force-induced skeletal remodeling. The results of this study showed that 47 well-documented proteins primarily function in many key changes related to the regulation of signal transduction events. For example, fibronectin 1 (FN-1) is localized on the extracellular matrix (ECM) and forms bonds with the focal adhesions constituting a primary pathway for intracellular force transmission initiating mechanosensing events [Chen, 2008]. FN-1 is formed in the early phase of osteogenesis and is maintained within mineralized matrix [Tang et al., 2004]. Laminin plays a regulatory role in cellular function through binding to various receptor proteins on the cell surface [Tzu

and Marinkovich, 2008]. In a novel signal transduction pathway, Gstp2 is activated by PenCB and contributes to the stimulation of GSTP1 expression [Abel et al., 2004]. Cdc42 controls signal transduction pathways that are essential for cell growth [Olson et al., 1995]. TR is a member of a recently identified class of signaling factors that use critical cysteine motif(s) to act as redox-sensitive “sulphydryl switches.” These switches reversibly modulate specific signal transduction cascades, and regulate downstream proteins with similar redox-sensitive sites [Smart et al., 2004]. Cdc 10/ankyrin repeat region within the intracellular domain plays an essential role in postulated signal transduction events [Rebay et al., 1993]. The bioinformatics analyses suggest that 28 proteins have not been identified in the skeletal remodeling process. Functional studies are required to identify the role of these proteins.

In our study, tropomyosin 4 appeared to be strongly up-regulated by mechanical force (label-free result: fold change = 4.5084, *P*-value = 0.0057). Tropomyosin 4 is a member of the large family of actin-binding regulatory proteins that are expressed in non-muscle cells. To date, no direct effects of mechanical force on tropomyosins have been reported. Tropomyosin 4 might influence bone metabolism either by affecting bone resorption or bone formation. To initiate bone resorption, osteoclasts must polarize and directly attach to the bone surface by specific adhesion structures called podosomes, which have a high cytoskeleton protein turnover and are involved in osteoclast migration, adhesion, and resorption [McMichael and Lee, 2008]. Tropomyosins are involved in the stimulatory effect of simvastatin on bone formation in cultured mouse calvarial cells [Hwang et al., 2004]. A tropomyosin isoform is involved in the activation of tropomyosin-related kinases (TRK) proto-oncogene, which plays a role in endochondral and intramembranous ossification [Aiga et al., 2006]. The level of tropomyosin 4 was higher in the force treatment group indicating that tropomyosin 4 might play a role in both bone formation and resorption and that it is involved in skeletal tissue remodeling. Further functional studies are required to elucidate the role of tropomyosins in modulating the effects of mechanical force on skeletal tissue resorption and formation.

This study offers a starting point for elucidating the pleiotropic effects of mechanical force on skeletal tissue. Functional studies are in progress to clarify the physiological role of the identified proteins in the bone-sparing effect of mechanical force and to address their role within bone compartments.

ACKNOWLEDGMENTS

The work was supported by Jiangsu Province's Outstanding Medical Academic Leader program, a grant from the National Natural Science Foundation of China (30572068), a grant from Nanjing Medical University (NY0527).

REFERENCES

Abel EL, Opp SM, Verlinde CL, Bammler TK, Eaton DL. 2004. Characterization of atrazine biotransformation by human and murine glutathione S-transferases. *Toxicol Sci* 80:230–238.

Aiga A, Asaumi K, Lee YJ, Kadota H, Mitani S, Ozaki T, Takigawa M. 2006. Expression of neurotrophins and their receptors tropomyosin-related kinases (Trk) under tension-stress during distraction osteogenesis. *Acta Med Okayama* 60:267–277.

Chen CS. 2008. Mechanotransduction—A field pulling together? *J Cell Sci* 121:3285–3292.

Cravatt BF. 2005. Kinase chemical genomics a new rule for the exceptions. *Nat Methods* 2:411–412.

Czupalla C, Mansukoski H, Riedl T, Thiel D, Krause E, Hoflack B. 2006. Proteomic analysis of lysosomal acid hydrolases secreted by osteoclasts. *Mol Cell Proteomics* 5:134–143.

Faibis D, Ott SM, Boskey AL. 2006. Mineral changes in osteoporosis a review. *Clin Orthop Relat Res* 443:28–38.

Gao BB, Stuart L, Feener EP. 2008. Label-free quantitative analysis of 1D-PAGE LC/MS/MS proteome: Application on angiotensin II stimulated smooth muscle cells secretome. *Mol Cell Proteomics* 7:2399–2409.

Hou B, Fukai N, Olsen BR. 2007. Mechanical force-induced midpalatal suture remodeling in mice. *Bone* 40:1483–1493.

Huiskes R, Ruimerman R, Lenthe van GH, Janssen JD. 2000. Effects of mechanical forces on maintenance and adaptation of form in trabecular bone. *Nature* 405:704–706.

Hwang a, Lee EJ, Kim MH, Li SZ, Jin YJ, Rhee Y, Kim YM, Lim SK. 2004. Calcyclin, a Ca²⁺ ion-binding protein, contributes to the anabolic effects of simvastatin on bone. *J Biol Chem* 279:21239–21247.

Ma JQ, Wu YX, Zhang WB, Smales RJ, Huang Y, Pan Y, Wang L. 2008. Up-regulation of multiple proteins and biological processes during maxillary expansion in rats. *BMC Musculoskeletal Disord* 9:37. 10.1186/1471-2474-9-37.

McMichael BK, Lee BS. 2008. Tropomyosin 4 regulates adhesion structures and resorative capacity in osteoclasts. *Exp Cell Res* 314:564–573.

Nikitin A, Egorov S, Daraselia N, Mazo I. 2003. Pathway studio the analysis and navigation of molecular networks. *Bioinformatics* 19:2155–2157.

Olson MF, Ashworth A, Hall A. 1995. An essential role for Rho, Rac, and Cdc42 GTPases in cell cycle progression through G1. *Science* 269:1270–1272.

Piltti J, Häyrynen J, Karjalainen HM, Lammi MJ. 2008. Proteomics of chondrocytes with special reference to phosphorylation changes of proteins in stretched human chondrosarcoma cells. *Biorheology* 45:323–335.

Pollard HB, Eidelman O, Jozwik C, Huang W, Srivastava M, Ji XD, McGowan B, Norris CF, Todo T, Darling T, Mogayzel PJ, Zeitlin PL, Wright J, Guggino WB, Metcalf E, Driscoll WJ, Mueller G, Paweletz C, Jacobowitz DM. 2006. Denovo biosynthetic profiling of high abundance proteins in cystic fibrosis lung epithelial cells. *Mol Cell Proteomics* 5:1628–1637.

Raisz LG. 1999. Physiology and pathophysiology of bone remodeling. *Clin Chem* 45:1353–1358.

Rebay I, Fehon RG, Artavanis-Tsakonas S. 1993. Specific truncations of Drosophila Notch define dominant activated and dominantnegative forms of the receptor. *Cell* 74:319–329.

Rubin J, Rubin C, Jacobs CR. 2006. Molecular pathways mediating mechanical signaling in bone. *Gene* 367:1–16.

Smart DK, Ortiz KL, Mattson D, Bradbury CM, Bisht KS, Sieck LK, Brechbiel MW, Gius D. 2004. Thioredoxin reductase as a potential molecular target for anticancer agents that induce oxidative stress. *Cancer Res* 64:6716–6724.

Tang CH, Yang RS, Huang TH, Liu SH, Fu WM. 2004. Enhancement of fibronectin fibrillogenesis and bone formation by basic fibroblast growth factor via protein kinase C-dependent pathway in rat osteoblasts. *Mol Pharmacol* 66:440–449.

Tzu J, Marinkovich MP. 2008. Bridging structure with function: Structural, regulatory, and developmental role of laminins. *Int J Biochem Cell Biol* 40:199–214.

Wang D, Park JS, Chu JS, Krakowski A, Luo K, Chen DJ, Li S. 2004. Proteomic profiling of bone marrow mesenchymal stem cells upon transforming growth factor beta1 stimulation. *J Biol Chem* 279:43725–43734.

Wu CC, Yates JR III. 2003. The application of mass spectrometry to membrane proteomics. *Nat Biotechnol* 21:262–267.

Xie C, Ye M, Jiang X, Jin W, Zou H. 2006. Octadecylated silica monolith capillary column with integrated nanoelectrospray ionization emitter for highly efficient proteome analysis. *Mol Cell Proteomics* 5:454–461.

Zeeberg BR, Feng W, Wang G, Wang MD, Fojo AT, Sunshine M, Narasimhan S, Kane DW, Reinhold WC, Lababidi S, Bussey KJ, Riss J, Barrett JC, Weinstein JN. 2003. GoMiner: A resource for biological interpretation of genomic and proteomic data. *GenomeBiology* 4:R28.